Efficient production of hybrid bio-nanomaterials by continuous microchannel emulsification: Dye-doped SiO_2 and Au-PLGA nanoparticles

Ane Larrea,[a#] Alberto Clemente[a#] , Edurne Luque-Michel[c,d] and Victor Sebastian[a,b]*

[a].Institute of Nanoscience of Aragon (INA) and Department of Chemical, Engineering and Environmental Technology, University of Zaragoza, C/ Mariano Esquillor, s/n, I+D+i Building, 50018, Zaragoza, Spain.; Tel: +34 876555441; Fax: +34 976 761879. E-mail: victorse@unizar.es.

[b].CIBER de Bioingeniería, Biomateriales y Nanomedicina (CIBER-BBN), Centro de Investigación Biomédica en Red. C/ Monforte de Lemos 3-5, Pabellón 11, 28029 Madrid.

[c].Department of Pharmacy and Pharmaceutical Technology. School of Pharmacy, University of Navarra, C/ Irunlarrea 1, E-31008 Pamplona, Spain. Tel: + 34 948 425 600 ext. 6519; Fax: + 34 948 425 649 e-mail: mjblanco@unav.es

[d].IdiSNA, Fundación Instituto de Investigación Sanitaria de Navarra

KEYWORDS: Microchannel emulsification, hybrid nanomaterials, microfluidics, bio-nanomaterials, continuous production

ABSTRACT. A novel microfluidic system was designed to produce in a continuous manner hybrid nanomaterials using the microchannel double w/o/w emulsification technique. Double w/o/w nanoemulsions were produced combining two inter-digital micromixers that afford working in continuous flow and with a high reproducibility and control on the reaction conditions. High throughput production of two hybrid nanomaterials, Dye-doped SiO_2 (4 mg/min) and Au-loaded Poly(lactic-co-glycolic) acid (PLGA) (168 mg/min) nanoparticles, was achieved, showing the resulting nanomaterials excellent and reproducible optical properties and tunable loading. These hybrid nanomaterials could be potentially used in different biomedical applications. In addition, the microfluidic system designed for carrying out double emulsification enabled to decrease the particle size distribution of Dye-doped SiO_2 nanoparticles (NPs) up to 20 nm and to improve the Au NPs loading efficiency in Au-loaded PLGA hybrid nanoparticles. The excellent control achieved in the Au NPs loading allowed tuning the payload on demand. Finally, the microfluidic system designed in this work overpasses the productivity described in previously published batch-type reactors, while assuring the same properties of the resulting hybrid nanomaterials.

INTRODUCTION

The continuous advance of nanomaterials science and its unprecedented application in more than 1,800 nanotechnology-based consumer products [1], indicate that nanomaterials are crucial to develop new applications: biological tagging [2, 3], medical diagnostics and treatment [4-6], solar energy harvesting [7] catalysis[8, 9] and electro-optical applications [10, 11].

Hybrid and multifunctional nanomaterials attain new properties by combining several materials on the same nanosystem, achieving, in some cases, even synergetic properties. However, some of the nanomaterials must be synthesized maintaining a sophisticated

configuration (core/shell, hollow structure, nanoalloy, etc.…) to fulfil the required specifications. The strict requirements on the characteristics of these nanomaterials pose serious challenges to their mass production [12]. This fact is largely attributed to the complex, multistep batch laboratory procedures that are not amenable to large-scale production.

The stages governing nanocrystals formation are highly sensitive to experimental details such as the way as reagents are introduced and mixed, stirring rate and heat transfer. This implies that to scale up a synthesis by simply increasing the volume of the reaction solution is just unfeasible [13]. Furthermore, it is challenging to achieve batch-to-batch reproducibility. Then, it seems obvious that the scale-up production in batch reactors is not amenable by increasing the reaction volume, and it should be performed by adapting the synthesis to a continuous process.

Emulsification is considered one of the nanomaterial production techniques with the highest size control reachable over the produced nanomaterials. This control is achieved by the formation of monodisperse micelles and vesicles that contain a representative amount of reagents and behave as individual nanoreactors. Highly energetic homogenization techniques such as probe sonication have been used to effectively produce tiny nanoparticles [14]. However, the sonication process presents a serious limitation for scaling-up the production [15]. As the intensity of the ultrasound in a liquid decreases rapidly with the distance to the sonotrode, larger volumes may not be well homogenized, providing a heterogeneous distribution of acoustic waves and consequent NPs polydispersity[15].

Emulsification can also be produced in high-pressure valve homogenizers, static mixers and mechanically stirred systems, where a pre-emulsion is forced to pass through a high shear region to disrupt large droplets into smaller ones. However, the resulting droplets are highly polydisperse due to a non-homogenous distribution of shear stress[16]. Microengineering

techniques address the limitations of conventional emulsifiers by controlling the location and distribution of shear stress. This fact can afford to achieve monodisperse droplets of tunable size. The production of droplets is generated through microchannels, where mean drop size is controlled by tuning a wide variety of variables: system geometry, hydrodynamic conditions, emulsion formulation, and microchannel wettability[15]. Microchannels integrated in microreactors can have a plethora of geometries that ease the contact between the continuous and dispersed phases to generate drops (i.e.,T junctions, cross junctions, Y junctions and flow focusing devices)[16]. Continuous flow microreactors integrate heaters and fluid control elements that offer a solution to scale-up challenges and enable the multi-stage processing [17]. Microreactors present inherent advantages, including enhancement of mass and heat transfer, feedback control of temperature and feed streams, good synthesis reproducibility, and low reagent consumption during optimization [18]. In addition, the small reaction volumes combined with the high heat and mass transfer rates enable to carry out fast kinetically-controlled reactions where the mixing time is shorter than the residence time.

Microchannel emulsification exploits the interfacial tension between non-miscible phases as the driving force for emulsion formation [19]. The high shear stress created at the microscale enables to deform and disrupt large droplets into smaller ones as a function of Laplace pressure, forming monodispersed emulsions. The production of microparticles by double emulsification in continuous flow is well-reported, but decreasing the particle dimension below the micrometer scale is challenging [15, 20]. Consequently, new synthesis approaches are still demanded [12]. To the best of our knowledge, no publications face the nanoscale production of materials by the double emulsification technique.

This work aims to show the versatility of a microfluidic platform based on the assembly of micromixers and microfluidic coils to achieve an excellent control in the continuous production of two types of hybrid nanomaterials by the microchannel emulsification technique. The synthesis of the selected nanomaterials is usually carried out in conventional batch reactors following multi-step processes, suffering from limited reproducibility and heterogeneity. We have adapted the batch production of dye-doped SiO_2 NPs and Au-polymer NPs to a continuous fashion procedure based on a double emulsification technique.

EXPERIMENTAL SECTION

Materials

Polymer poly (D,L-lactic acid/glycolic acid) 50:50 (PLGA; MW 38-54KDa), under the commercial name Resomer® RG 504 was purchased from Evonik Industries (Evonik Röhm GmbH, Germany). The surfactants sodium cholate hydrate (>99%) and Triton X100, and the synthesis reagents as gold (III) chloride hydrate (50% Au bases, $HAuCl_4.XH_2O$), sodium citrate dihydrate (≥99%, $C_6H_5Na_3O_7.2H_2O$), ethyl acetate (HPLC grade), fluorescein isothiocyanate isomer I (FITC, 90%), 3-Aminopropyl 3-Triethoxysilylpropylamine (APTES, 98%), tetraethyl orthosilicate (TEOS, 98%), ammonium hydroxide (25%), 1-hexanol (99%) and cyclohexane (99%) were purchased from Sigma Aldrich (St. Louis, MO, USA) and used without further purification. All references to water imply the use of Milli-Q water previously filtered through a 0.2 μm cellulose nitrate membrane.

Microfluidic Systems

Nanoparticles were prepared using two consecutive slit-interdigital micromixers with an inner volume of 8 μL (Micro4Industries GmbH, Mainz, Germany) interfaced with one

Polytetrafluoroethylene (PTFE) microcoil tubing (OD=1/16″, ID= 1mm) (Figure 1-d,e). Slit-interdigital micromixers follow the principle of producing thin liquid lamellae, guiding them in contact through a flow-through-chamber. The continuous and dispersed phase streams were splitted into 16 substreams of 45 μm width. Substreams were later on recombined to increase the contact surface between the two immiscible phases to produce the emulsification process. The length of the PTFE coil was adapted to the residence time required. Inlet streams in the microfluidic system were labeled as F1, F2 and F3, being F1 and F2 mixed in the first micromixer and this resulting stream mixed with F3 in the second micromixer. Reagents were injected using three syringe pumps (Harvard Apparatus, Holliston, MA, USA). A water temperature-controlled bath was set to activate the silica growth or the reduction of Au^{3+} ions.

Continuous FITC-SiO_2 NPs Synthesis Procedure

Firstly, a FITC-APTES conjugate was synthesized following Santra's procedure [21]. 10.6 mg FITC and 0.146 mL APTES were added to a 2 mL ethanol volume, and stirred under an inert atmosphere and in the absence of light during 12 hours. F1 stream carries an aqueous solution of 25.5 mL TX-100 (74.2%v), 3 mL TEOS (8.7%v), 4.35 mL water (12.7%v) and 1.5 mL of FICT-APTES solution (4.4%v) (Figure 1 and Figure S1). F2 stream carries the oily phase, consisting on 99 mL cyclohexane (82.8%v) and 20.57 mL of 1-hexanol (17.2%v). The two phases were injected into the micromixer by two syringe pumps, where the microemulsion was formed. A third stream F3, carrying an aqueous solution of 51 mL TX-100 (74.2%v), 6 mL NH_4OH 25% (8.7%v) and 11.7 mL Milli-Q water (17.0%v), was introduced to the stream before the growth coil. Flow rates and concentrations were adjusted to keep the same molar ratios of the conventional synthesis method. F1 and F3 were set with a flow rate of 0.36 mL/min, whereas F2 was fed at 0.108 mL/min. After synthesis, the microemulsion was destabilized by adding a

water-alcohol mixture (86% ethanol, 5% propanol, 5% methanol, 4% water), and centrifuged at 10,000 rpm during 12 minutes. Prior to the fluorescence measurements, the samples were centrifuged and rinsed with fresh Milli-Q water. Prior to sampling, the microemulsion was destabilized by adding a water-alcohol mixture (86% ethanol, 5% propanol, 5% methanol, 4% water), and centrifuged at 10,000 rpm during 12 minutes. The instrument used was a Perkin Elmer LS55 spectrofluorometer, equipped with a Xenon discharge lamp, using an excitation wavelength of 490 nm. Batch type synthesis of FITC-SiO_2 NPs was carried out following Santra's procedure [21].

Continuous production of PLGA-Au hybrid Nanoparticles

Au-loaded PLGA Nanoparticles were prepared as follows:

F1 stream is the internal aqueous phase and consisted of 0.1 - 0.5% (w/v) chloroauric acid and sodium citrate, with a molar ratio chloroauric acid| sodium citrate of 1|5, dissolved in 10 mL of water. The organic stream F2 was prepared by adding 0.5-1.25 %(w/v) of polymer PLGA (50:50) in 20 mL of ethyl acetate. F1 and F2 were injected in the first micromixer with a flow rate of 4.5 and 13.5 mL/min, respectively.

The resulting primary emulsion produced after mixing F1 and F2 was continuously pumped in the second micromixer to form the secondary emulsion with the aid of the F3 stream (Figure 1-e). F3 stream was prepared by dissolving Sodium Cholate 1% (w/v) in 50 mL of Milli-Q water, and injected at a flow rate of 36 mL/min.

Both micromixers were placed in an ice-water bath to set the emulsification temperature at 17ºC. After the formation of a stable emulsion, the encapsulated gold was reduced using two approaches: (1) Batch reduction; which is a semi-continuous approach where the final emulsion was introduced in a closed vessel and heated at 45 ^{o}C during 20 minutes under magnetic stirring.

(2) µfluidic reduction, where the final emulsion was pumped at a flow rate of 124 µl/min across a PTFE tube (0.04" i.d. and 5 feet length) located in a heated bath at 45 ^{o}C, setting a residence time of 10 minutes.

Finally, the same volume of sodium cholate 0,3% (w/v) was added to the reduced emulsion. The organic solvent was evaporated under continuous stirring (600 rpm) in an open flask during 3 hours.

Hybrid nanomaterials characterization

Determination of NP morphology. Electron microscopy observations were carried out at the LMA-INA-Universidad Zaragoza facilities. Scanning electron microscopy (SEM, Inspect F50, FEI, Eindhoven, The Netherlands) was employed to determine the morphology of the synthesized NPs. The freshly prepared colloidal nanoparticles were mixed during 1.5 hours with the same volume of phosphotungstic acid solution (7.5% w/v) used as staining agent. The dispersion was centrifuged and washed three times with Milli-Q water and later re-suspended. A drop of the resulting nanoparticle suspension was placed on a glass slide, air dried and sputtered with platinum under vacuum before SEM observation.

Transmission electron microscopy observations were carried using a T20-FEI microscope with a LaB6 electron source fitted with a "SuperTwin®" objective lens allowing a point-to-point resolution of 2.4 Å. A 2.5 µL suspension of stained PLGA NPs was pipetted onto a TEM copper grid having a continuous carbon film. Samples were let to evaporate completely and then analyzed. Aberration corrected scanning transmission electron microscopy (Cs-corrected STEM) images were acquired at LMA-INA-UNIZAR using a high angle annular dark field detector in a FEI XFEG TITAN electron microscope operated at 300 kV equipped with a CETCOR Cs-probe corrector from CEOS Company allowing formation of an electron probe of 0.08 nm.

Size and Size Distribution measurement. Nanoparticle size and size distributions were determined by Dynamic Light Scattering (Zeta Plus, Brookhaven Instruments Corporation, NY) after appropriate dilution with Milli-Q water. At least five replicate measurements were recorded in each case.

*Laser Irradiation***.** Irradiation experiments were performed with a collimated light at 532 nm and power density of 4.2 W/cm^2. Measurements were carried out in 24-cell culture insert plates made of polycarbonate and with a fixed volume of 1 mL of dispersion. The distance between the laser head and the sample was approximately 1 cm. In all the assays the sample concentration used was 0.24 mg/mL of gold and 1.25 mg/mL of PLGA.

RESULTS AND DISCUSSION

This section is structured in two subsections that summarize the most relevant results obtained in the continuous production of two hybrid nanomaterials: FITC-SiO_2 NPs and Au-loaded PLGA NPs. In addition to the microfluidic production, both types of hybrid nanomaterials were also produced in conventional batch type reactors with the assistance of an ultrasound sonotrode. In addition to the aforementioned shortcomings of conventional reactors to operate in multi-step process reactions, we observed a remarkable limitation of performing the emulsification process with the sonotrode. Figures 1 a and b depict the surface of the sonotrode tip. Figure 1-a shows a pristine tip before any ultrasound treatment. However, the appearance of the sonotrode tip only after certain ultrasound treatments reveals that the cavitation generated during the ultrasonic emulsification can etch the tip surface. Consequently, ions or particles from the sonotrode tip could be emitted into the product by cavitational abrasion of the sonotrode itself since it consists of metallic alloys, promoting a feasible product contamination. This phenomenon could be

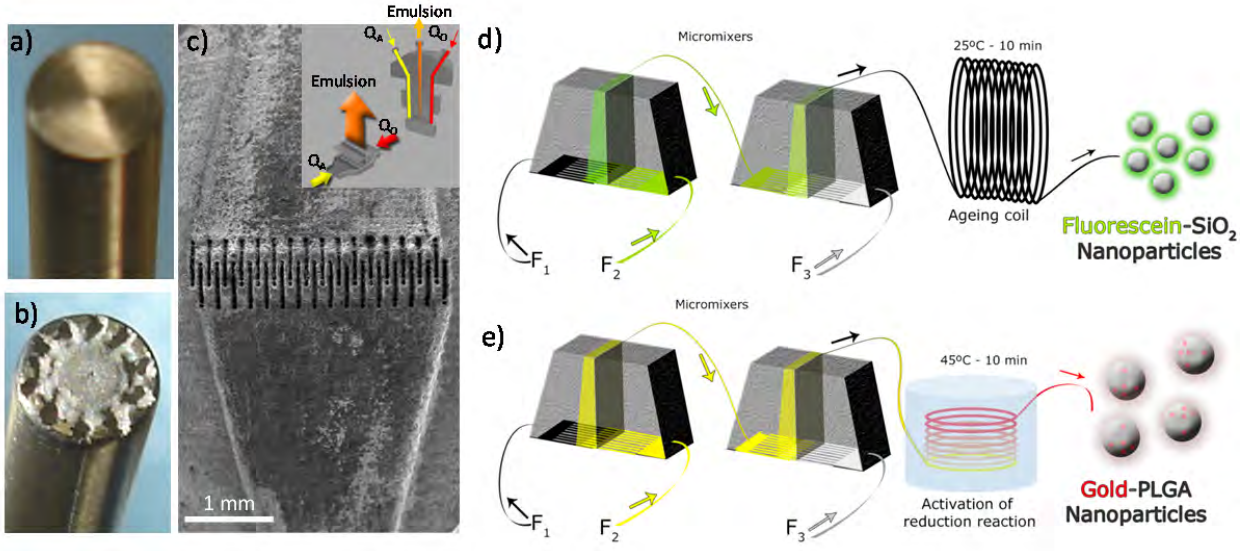

Figure 1.- a) Optical image of an unused sonotrode. b) Optical image of the sonotrode after suffering cavitational abrasion, c) SEM image of the microfluidic interdigital mixer used to produce the nanomaterials by microchannel emulsification. d) Schematic representation of the continuous three-stage microfluidic system to produce Fluorescein-SiO_2 nanoparticles. Two micromixers and an ageing coil (ID 800 μm) were used to achieve the emulsification and condensation of silica precursors as well as the encapsulation of fluorescein, respectively. F1 contains the aqueous phase, with TEOS, FITC-APTES conjugate and TX-100. F2 carries the oily phase, with cyclohexane and 1-hexanol. After the microemulsion is formed in the micromixer, F3 introduces NH_4OH 25%, acting as the catalyst for the TEOS and APTES hydrolysis. e) Schematic representation of the continuous three-stage microfluidic system to produce hybrid Au-loaded PLGA nanoparticles. Two micromixers and a heated coil were used to achieve the emulsification of PLGA and Au NPs encapsulation, respectively. F1 contains PLGA and ethyl acetate, F2 is composed of chloroauric acid and sodium citrate dissolved in Milli-Q water, and F3 contains sodium cholate and Milli-Q water.

serious if the produced nanomaterials are aimed to be used in biomedical applications, as it occurs in this case, and it has been noticed by other authors working in the field [22]. However,

there were no documented data to qualitatively estimate this abrasion phenomenon. Then, we consider that new emulsification approaches must be developed to assure not only a fine control in the synthesis conditions, but also free of cross-contamination. Considering these facts, we proposed a microfluidic system as an alternative approach to produce emulsions without metal contamination. The shear stress produced at the interphase of immiscible liquid microflows is energetic enough to achieve the emulsion formation without the need of external mechanical or ultrasonic forces[15]. In addition, there is no cavitation, avoiding abrasion phenomenon and emulsion contamination.

Production of dye-doped nanoparticle probes

Dye-doped nanoparticle probes (i.e., Cornell dots) have shown an excellent potential in bioimaging since they can carry many fluorescent molecules to enhance the detection sensitivity [23]. In addition, the encapsulation of fluorescent molecules within ceramic or polymeric matrixes reduces their exposure to intracellular media, preventing adverse photobleaching reactions, while exposing a biocompatible an easily functionalizable surface [24-27]. Silica is a suitable material for this purpose since it exhibits good mechanical and chemical stability; it is easily dispersible in aqueous solutions and is optically transparent [24, 28]. However, the application of these nanoparticles in cellular and biological applications requires achieving a particle size as small as possible [23].

Fluorescein-doped silica NPs are generally synthesized in a batch type reactor by the water in oil micro-emulsion technique. This procedure enabled to produce monodisperse nanoparticles with a mean particle size of 65±4 nm (Figure 2-a) [21]. The formation of micro-emulsions in batch reactors limits the amount of reactants within the micro-micelles, resulting on a better particle-size distribution than the ones obtained for particles resulting from the batch method

without emulsification [29]. However, our efforts to decrease the particle size under the reported batch-procedure threshold were unsuccessful. Then, we decided to produce this type of NPs using the same chemical procedure than the protocol reported by Santra et al. [21], but using the microchannel emulsification approach.

As depicted in Figure 1-c, a slit interdigital micromixer (microchannels width= 45 μm) was selected to create a high shear-stress by multi-lamination of the reagent immiscible streams. In addition, this micromixer retains a high surface area-to-volume ratio and excellent mixing characteristics which help to reduce or avoid temperature and concentration heterogeneities [15]. Figure 1-d shows the schematic representation of the microfluidic platform designed to produce fluorescein-doped SiO_2 nanoparticles. This microfluidic system is divided in three stages: 1) Micromixer 1-Emulsification of silica precursor and fluorescein conjugate (FITC-APTES), 2) Micromixer 2-Controlled addition of the ammonia as a basic catalyst for the hydrolysis and condensation process of the silica precursor [30], and 3) Microcoil- Nanoparticle growth by condensation of $Si(OH)_4$.

Silica precursor (TEOS) is hydrolyzed to form Si monomers, $Si(OH)_4$, that can polymerize (condensation reaction) under the presence of aqueous ammonia that has the role of catalyzing the formation of silica and the entrapment of FITC. Consequently, it is of paramount importance to control the interaction between TEOS and ammonia in order to tune the growth kinetics of silica nanoparticles, as well as the dimensions of the micelles where these reagents are located.

Flow rates, streams compositions, geometric dispositions, residence times and temperatures were modified to tune the resulting particle-size distribution. If ammonia was fed in the F1 stream (i.e., injected in the first micromixer), a fast silica condensation blocked the interdigital micro-channels and a continuous production of dye-silica nanoparticles was not affordable.

Then, in a second approach, ammonia was downstream injected in an additional micromixer to promote the controlled diffusion into the micelles. Synthesis of SiO_2 NPs was previously studied in microfluidics systems using the well-known Stöber method. This microfluidic approach enabled to achieve monodisperse SiO_2 colloids over 100 nm size at a residence time ranging between 15 and 30 minutes [31, 32]. Then, we proposed in this work to accelerate the SiO_2 condensation by increasing the synthesis temperature[32]. Figure 2-b depicts the morphology of the dye-doped SiO_2 NPs produced in a continuous fashion at 65 ^{o}C with only 10 minutes residence time. The particle size distribution was heterogeneous, inferring that the emulsion was not properly formed at those studied conditions.

According to previous results, the temperature of reagents during the mixing stage controls the microchannel emulsification process since there is a balance between the viscous shear stress and the surface tension to obtain an homogenous emulsion [15]. Consequentially, the synthesis of dye-doped SiO_2 NPs was further studied at room temperature (RT) to promote both the formation of a stable emulsion and the hydrolysis /condensation of TEOS at a residence time as short as possible. The most outstanding results were achieved after mixing the inlets streams at RT with 3 minutes residence time in the growth stage (microcoil), producing homogenous dye-doped SiO_2 NPs with a mean particle size of 19.2±4.7 nm (Figure 2-c and Figure S2). Particle size was statistically determined by measuring no less than 100 NPs from TEM images. These nanoparticles were maintained under stirring in the collection flask at several ageing times (10, 30 and 90 minutes), and TEM samples were taken to observe if the resulting NPs evolved. Further TEM analysis showed that after 90 minutes, the mean particle size was 22±4.1 nm (Figure 2-d), indicating that the reaction was essentially complete in the microfluidic system under the 3 minutes residence time. The residence time was decreased to 1 minute by increasing

by three fold the total flow rate (Figure 2-e and Figure S2). However, the particle-size distribution of the resulting NPs was heterogeneous in this case, obtaining nanoparticles with a mean particle size ranging from 10 nm to 20 nm. This polydispersity obtained indicates that the fluorescein-doped SiO_2 NPs evolved in the collecting flask. Consequently, a residence time of 3 minutes was selected as the proper reaction time to promote a complete TEOS condensation into monodisperse NPs.

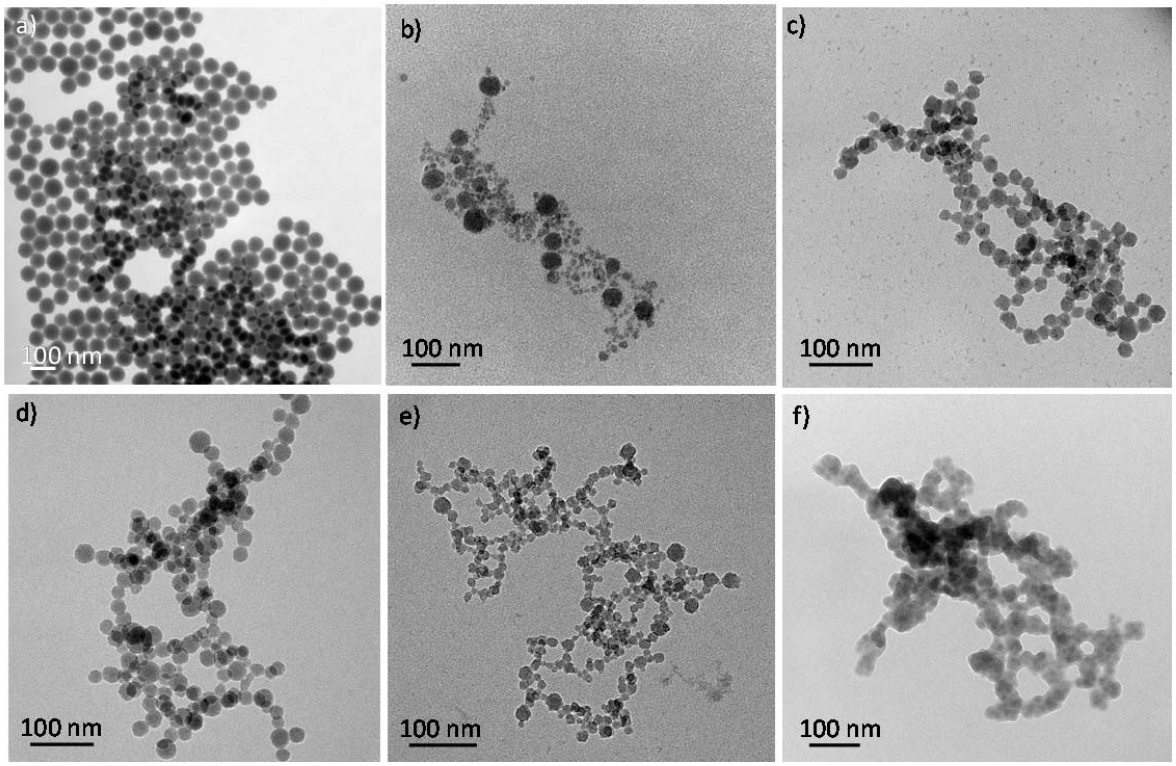

Figure 2.- TEM images of fluorescein-doped SiO_2 NPs. a) NPs produced in a batch type reactor during 24 hours at room temperature. TEM images of fluorescein-doped SiO_2 NPs produced by microchannel emulsification: b) Residence time = 10 minutes, T = 65 ^{o}C, c) Residence time = 3 minutes, room temperature, d) Residence time = 3 minutes, room temperature and 30 minutes aging in the collection flask, e) Residence time = 1 minute, room temperature. f) TEM images of fluorescein-doped SiO_2 NPs produced in a batch batch-type reactor, synthesis time = 3 minutes, room temperature.

Figure 2-f depicts the nanoparticles produced in the batch-type reactor at the same conditions (temperature and time) than the ones obtained with the microfluidic system. It can be inferred from the TEM images that the particles morphology is not well defined as a result of the slow TEOS condensation rate. These results are in full agreement with previous reported results [32] where SiO_2 NPs grew faster in microreactors than in batch reactors at similar synthesis conditions. The confinement of reagents in nanoscale vesicles (nanoemulsion) enables a fast crystallization rate, but still preserving an excellent control in the nucleation and growth stages to produce monodisperse nanoparticles. Then, this microfluidic emulsification approach reduces the synthesis time and accelerates the silica growth from the reported 15 minutes (traditional Stöber method in microfluidics) [32] to just 3 minutes, with an approximate productivity of 4 mg/min.

In addition, there is a remarkable reduction in the nanoparticle sizes from 67 nm in batch-type reactor to 22 nm in the microfluidic system. This fact is remarkable to direct the application of these nanoparticles towards a biomedical use as imaging probes.

Finally, Figure 3 shows the fluorescent spectrum of dye-doped SiO_2 NPs produced by microchannel emulsification. Maximum emission for these nanoparticles was found at 515 nm. A comparison with free FITC-APTS conjugate and with nanoparticles prepared by the conventional method [24] shows the same emission pattern. Having fluorescein small stokes shift, lamp reflection can be seen as a saturation signal between 480 and 500 nm. UV-VIS analysis rendered a 20.5% labelling yield, with a 0.19% weight of FITC encapsulated in the silica nanoparticles.

In light of these results, a monodisperse production of fluorescein-doped 19-22 nm SiO_2 NPs was achieved in a residence time as short as 3 minutes. The most interesting feature is that the

particle size was threefold decreased from the previously reported data (67 nm), while retaining the fluorescent emission and increasing the production rate 500 times as compared to the reported batch processes, typically conducted in 24 hours [21]. Without a doubt, these achievements will improve the translation of fluorescein-doped silica to any biomedical imaging applications.

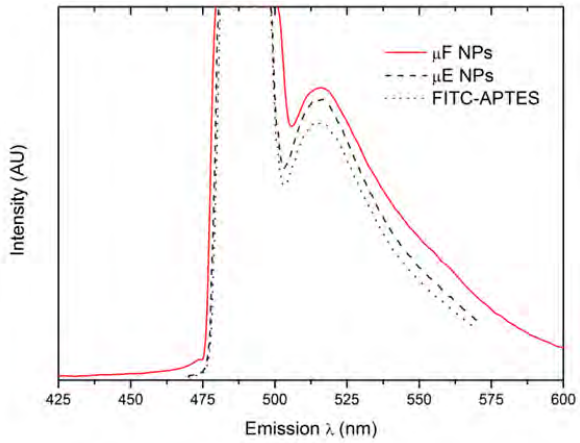

Figure 3: Fluorescence emission spectra of FITC-doped SiO_2 NPS produced by microfluidic (μF NPs), FITC-doped SiO_2 NPs produced by conventional methods (μE NPs) and free FITC-APTES conjugates. Measurement conditions were 490 nm excitation wavelength, 7.5 nm monochromator slit width and 200 nm/s scan speed.

Production of Au loaded polymeric nanoparticles

Encapsulation of Au NPs in polymeric matrixes was selected as a potential nanocrystallization process to highlight the versatility of the proposed microfluidic platform. The methodology commonly used to prepare polymeric NPs by emulsification is directly related to the particle size and morphology. In addition, the encapsulation of metal NPs in polymeric NPs to produce hybrid materials for biomedical applications as theranostic agents is challenging[3]. We have currently developed a new encapsulation strategy based on the in-situ reduction of $AuCl_4^-$ ions inside the

polymeric matrix using batch type reactors [3]. Tetrachloroaurate and citrate ions were entrapped in poly(DL-lactic-co-glycolic acid)-PLGA NPs, that were prepared by a double emulsion (w/o/w) method [3]. The reduction of $AuCl_4^-$ ions by citrate can be activated on demand by controlling the temperature of the emulsion. Considering that citrate ions act as a weak reducing agent, the highest the temperature is, the fastest the reducing kinetics of $AuCl_4^-$ are.[3] This strategy exerts the advantage that Au precursor is reduced after its encapsulation, which assures a selective formation of Au NPs inside the PLGA NPs. However, the reduction temperature must be lower that the vitreous transition temperature of the PLGA polymer, 45–50 °C.[3] We selected 45°C as a suitable temperature to activate the redox reaction while keeping sufficient polymer rigidity to minimize the outward diffusion of the encapsulated chemicals. This reported procedure circumvents some of the weaknesses of previous metal NP encapsulation strategies and enables the selective encapsulation of Au NPs in PLGA nanoparticles with a 100% loading efficiency (Figure 4 a-b) [3]. However, our reported procedure is a multi-stage synthesis procedure that is carried out in a batch type reactor, where the production rate is limited and an excellent control of synthesis variables is required to assure good reproducibility. Consequently, the design of a continuous production procedure would be of high interest [12].

The selective loading of Au NPs inside of PLGA NPs is highly dependent on two crucial stages: Au precursors entrapping and $AuCl_4^-$ reduction rate. The use of strong reducing agents such as sodium borohydride did not able to match the loading of Au precursors in the double w/o/w emulsion and the chemical reduction of Au ions (Figure 4-c). The fast reduction kinetics achieved with $NaBH_4$ inhibited the encapsulation of $AuCl_4^-$ and Au NPs were located outward the emulsion. On the other hand, the presence of a weak reducing agent, such as citrate ions, enabled the reduction of $AuCl_4^-$ to Au^0 following a kinetic rate that is directly proportional to the

temperature. At room temperature the gold reduction by citrate ions is negligible, which is desired to reduce on demand the gold precursor once it is entrapped in the polymeric matrix. However, not only a control on the reduction rate is required but also the solvent diffusion from the w/o/w emulsion during the temperature-triggered reduction step.

The solvent evaporation method is a well-established procedure to form polymeric NPs by the evaporation of the organic solvent and consecutive shrinkage of the initial emulsion droplet [33]. At the end, the polymer dispersed in the emulsion droplet is not soluble in the aqueous media and precipitates as a nanoparticle. Surprisingly, Au NPs tend to crystallize outward the PLGA NPs if the activation of the $AuCl_4^-$ ions by the reduction reaction was conducted in an air-open reactor (Figure 4 d-e). On the contrary, Au NPs were well encapsulated inside the PLGA NPs if the reduction reaction was carried out in a gas-tight reactor. [3] It implies that the Au NPs entrapment is sensitive to the solvent (ethyl acetate) evaporation process. In an open reactor, since ethyl acetate and water are partially miscible, Au ions together with ethyl acetate could diffuse out the micelle due to a partial pressure driving force of ethyl acetate (31 kPa at 45 ^oC). On the contrary, if the heating stage is conducted in a gas-tight reactor where the equilibrium in the gas phase is reached, the solvent evaporation is inhibited or at least significantly diminished and $AuCl_4^-$ ions can still be retained inside the micelle. Once the ions reduction stage was performed, the Au-loaded PLGA NPs were obtained by the mentioned solvent diffusion process in an open reactor, but the Au NPs cannot diffuse out due to steric impediment through the polymeric nanofibers. Then, it seems that confining the $AuCl_4^-$ reduction reaction is crucial to success in the Au NPs encapsulation and microfluidic reactors are a versatile tool to avoid solvent evaporation during the heating stage because reagents are confined by microchannels.

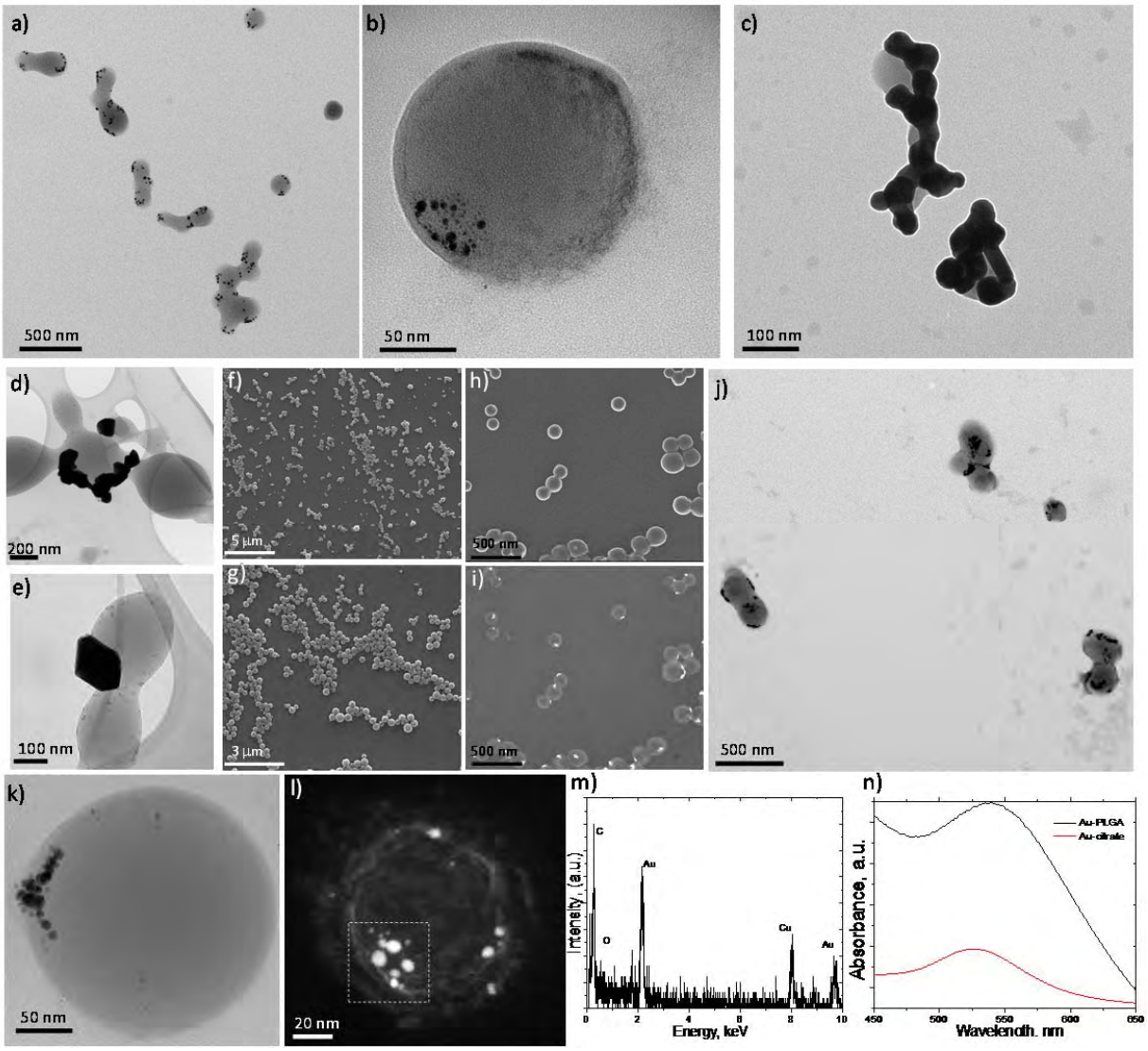

Figure 4.- Au-loaded PLGA hybrid NPs produced in w/o/w emulsion using batch type reactors. A) TEM image of Au- loaded PLGA NPs produced according to the procedure described by Luque-Michel at al. [3] b) TEM image of a representative Au-loaded PLGA NP, the dark contrast is associated to the location of Au NPs c) TEM image of Au- loaded PLGA NPs produced when sodium citrate was replaced by $NaBH_4$, d)-e) TEM images of Au- loaded PLGA NPs obtained if the temperature activated reduction of Au^{+3} ions is performed in an open-air reactor instead of a gas tight reactor. Au- loaded PLGA hybrid NPs produced in w/o/w emulsion using the microfluidic system, [PLGA] = 1.2 mg/mL PLGA/Au = 10 F1= 4,5 mL/min, F2= 13,5

mL/min, F3= 36 mL/min. f-h) SEM images of Au- loaded PLGA hybrid NPs, i) Back scattered electron micrograph to show the location of Au NPs in the same area as h), j) TEM image to show that Au is selectively encapsulated in PLGA NPs. k) TEM image of a representative Au-loaded PLGA NP, the dark contrast is associated to the location of Au NPs, l) HAADF-STEM micrograph of a representative Au- loaded PLGA hybrid NP to show by Z-contrast the location of Au NPs inside PLGA NPs, m) HAADF-EDS analysis of the area selected in l) to confirm the presence of a Au NPs, n) UV-VIS spectra of Au- loaded PLGA NPs and Au NPs as a reference.

Figure 1-e shows the microfluidic system used to produce hybrid Au-loaded PLGA nanoparticles in a continuous fashion. The microfluidic system is similar to the one used to produce dye-doped SiO_2 NPs, but the growth-condensation coil was substituted by a heating coil to activate the reduction of $AuCl_4^-$ ions by citrate ions. PLGA NPs entrapping tetrachloroaurate and citrate ions

were prepared by a double emulsion (w/o/w) method in continuous flow to afterwards reduce $AuCl_4^-$ ions into Au NPs in a microfluidic coil heated at 45 ^oC with a residence time of 10 minutes. The flow rates required to produce the polymer NPs (54 mL/min) by microchannel emulsification are larger than the ones used to form dye-doped SiO_2 NPs (0.82 mL/min) because of the high shear-stress required in the water-ethyl acetate system [15]. It implies that the NPs throughput is considerably improved with reference to the batch production.

Figures 4-f and 4-g depict SEM images at different magnifications of the Au- loaded PLGA NPs produced in continuous flow, obtaining spherical PLGA NPs with a relatively narrow particle-size distribution (192±58 nm, Figure S3). Fig. 4-h shows a SEM image obtained with secondary electrons where spherical PLGA NPs containing Au NPs are depicted. When the same PLGA NPs were analyzed through back-scattered electrons (Figure 4-i), the selective location of

Au NPs entrapped in PLGA NPs was observed. The Au entrapment in the NPs was also revealed by transmission electron microscopy (Figure 4-j,k). These images indicate that the location of Au NPs is close to the surface but they are still immersed in the PLGA matrix. This fact is in agreement with previous findings where electron microscopy images and pyrene fluorescence were used to elucidate the Au NPs location [3].

A further microscopy analysis from a single Au- loaded PLGA hybrid NP, using a STEM microscope with HAADF detector sensitive to the atomic number and the energy-dispersive X-ray spectroscopy analysis (EDS) on the brightest NPs, confirmed the location of Au NPs embedded in the PLGA matrix (Figure 4 l-m). Finally, the UV-Vis characterization showed the characteristic surface plasmon resonance peak of Au nanoparticles produced by citrate method (Figure 4-n).

The mean particle size was mainly sensitive to different parameters such as temperature, residence time, F1-F2-F3 flow rate ratios and polymer concentration. Figure 5 depicts some representative SEM images and the particle size distribution histograms of PLGA nanoparticles produced in continuous flow at different synthesis conditions. The residence time is a key variable to assure a high shear stress during the emulsification process. When the flow rate of F1, F2 and F3 was proportionally decreased from a total flow rate of 54 mL/min to 36 mL/min, the mean particle size increased up to 568 nm, obtaining a wide nanoparticle-size distribution. On the other hand, the PLGA polymer concentration has a significant effect in controlling the particle size. It was observed that the mean particle size was smaller in the experiments carried out with a low content of PLGA (Figure 5-b,c). This result is in agreement with some previous works obtained in batch type reactors [34, 35] which was attributed to an increase of the

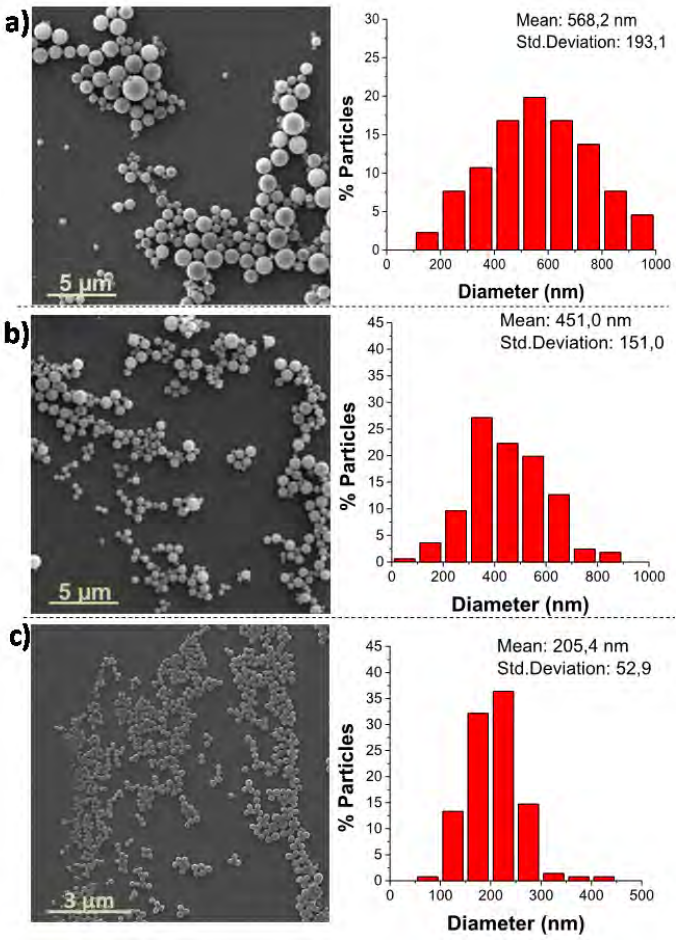

Figure 5.- SEM micrographs and particle size distribution histograms of PLGA NPs produced by double emulsion w/o/w emulsification at different conditions: a) [PLGA] = 6,2 mg/mL w/v_{total} F1= 3 mL/min, F2= 9 mL/min, F3= 24 mL/min (Q_{total} = 36 mL/min).b) [PLGA] = 6,2 mg/mL w/v_{total}. F1= 4,5 mL/min, F2= 13,5 mL/min, F3= 36 mL/min (Q total = 54 mL/min).c) [PLGA] = 1,2 mg/mL w/v_{total} F1= 4,5 mL/min, F2= 13,5 mL/min, F3= 36 mL/min (Q total = 54 mL/min).

viscosity with the increase in the PLGA concentration. This reduces the net shear stress during the emulsification process and results in the formation of droplets with larger size.

The gold NPs payload can be tuned according to the gold precursor concentration injected in the stream F2 (see scheme in Figure 1-e). Figure 6 a-c and Figure S4 depict the Au- loaded PLGA hybrid NPs produced when the PLGA/Au wt. ratio was ranged from 26 to 5. The density of Au NPs entrapped is directly proportional to the concentration of the $AuCl_4^-$ aqueous phase entrapped inthe w/o/w double emulsion. The synthesis throughput was increased by increasing the concentration of reagents, obtaining a productivity of Au- loaded PLGA hybrid NPs of up to 2.8 mg/s.

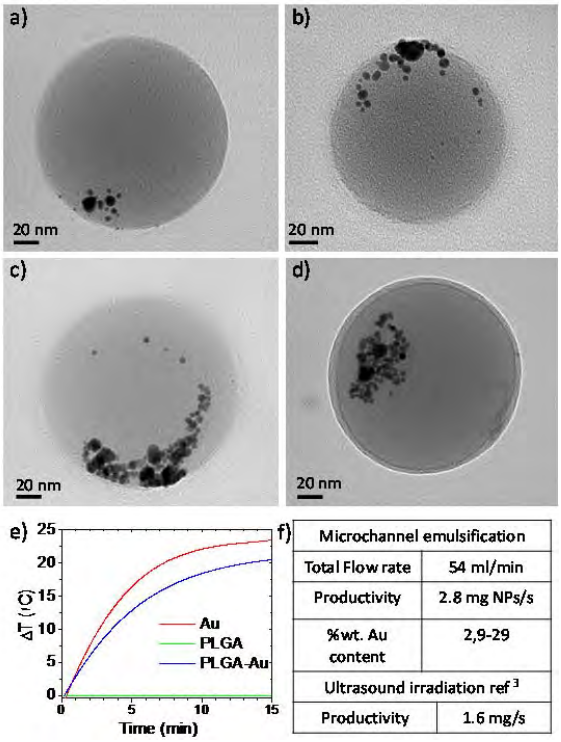

Microchannel emulsification	
Total Flow rate	54 ml/min
Productivity	2.8 mg NPs/s
%wt. Au content	2,9-29
Ultrasound irradiation ref [3]	
Productivity	1.6 mg/s

Figure 6.-TEM images of Au- loaded PLGA hybrid NPs produced with different $HAuCl_4$/PLGA ratios: a) [PLGA] = 1.2 mg/mL wt. PLGA/Au = 26 b) [PLGA] = 1.2 mg/mL wt. PLGA/Au = 10 c) [PLGA] = 1.2 mg/mL wt. PLGA/Au = 5 d) [PLGA] = 3.1 mg/mL wt. PLGA/Au = 10 e) Temperature increase as a function of time under laser irradiation (λ = 532 nm and power density of 4.2 W/cm^2) of Au NPs, PLGA NPs and the hybrid Au– loaded PLGA NPs. [Au] = 0.24 mg/mL. f) Comparison between microchannel and ultrasonic emulsification techniques.

(Figures 6-d). These findings and the fact that no Au NPs were located in the continuous phase confirm the exquisite encapsulation control achieved with the microfluidic system.

The hybrid Au loaded PLGA NPs produced by microchannel emulsification were exposed to continuous illumination to confirm their optoelectronic properties and to demonstrate that they can act as efficient light absorbers. The exposure of aqueous suspensions of Au– loaded PLGA NPs to continuous illumination at a laser power of 4.2 W/cm^2 (wavelength 532 nm) for 15 minutes resulted in a similar heating performance that the one achieved when aqueous dispersions of Au NPs, containing the same nominal Au loading, were subjected to irradiation (Figure 6e). On the other hand, a blank experiment with PLGA NPs without Au NPs inside showed temperature increases around 1°C only under the same conditions. These results clearly indicate that the Au encapsulated in the hybrid PLGA NPs are efficient light absorbers.

The fine control achieved in Au- loaded PLGA NP production using microfluidics implies that the use of two micromixers not only enables to form w/o/w emulsions with a controlled size at the nanometer scale, but also to control the NPs payload. In addition, microchannel emulsification enables to achieve a higher productivity (2.8 mg PLGA/s) than the one obtained with a batch type process (1.6 mg/s) [3] (Figure 6-f). Finally, the proposed microfluidic system facilitates the multistep processing, avoiding the diffusion of $AuCl_4^-$ ions in w/o/w emulsions during the thermal treatment.

CONCLUSIONS

A new microfluidic system was developed to produce hybrid nanomaterials potentially used in biomedical applications using a continuous fashion. The novelty of the proposed microfluidic system is that it enables a high throughput production of w/o/w emulsions under micrometer scale. The production of these nanomaterials is complex in batch type reactors since they are

obtained following multi-stage processes, suffering from low reproducibility. In this work, the production of these hybrid materials has been attempted showing high throughput and excellent control during the emulsion formation and nucleation/growth. Production of monodisperse dye-doped silica NPs was achieved with a mean particle size of 20 nm, facing the size limitation control of batch-type reported procedures. PLGA NPs were produced by a double emulsion w/o/w process without the assistance of high energy sources such as ultrasound waves. Au NPs were selectively encapsulated in PLGA NPs with 100% efficiency, controlling the most crucial stages: the reduction of $AuCl_4^-$ ions and solvent evaporation.

ASSOCIATED CONTENT

Supporting Information. Supporting figures are included

AUTHOR INFORMATION

victorse@unizar.es

# These authors contributed equally

ACKNOWLEDGMENT

This work has been carried out in the framework of the People Program (CIG-Marie Curie Actions, REA grant agreement no. 321642) .The Government of Aragon and the European Social Fund are gratefully acknowledged. CIBER-BBN is an initiative funded by the VI National R&D&i Plan 2008–2011 financed by the Instituto de Salud Carlos III with the assistance of the European Regional Development Fund. We thank Manuel Arruebo for his suggestions and helpful discussions.

REFERENCES

[1] http://www.nanotechproject.org/cpi/search-products/,
[2] L. Li, T.J. Daou, I. Texier, T.K.C. Tran, Q.L. Nguyen, P. Reiss, Highly Luminescent CuInS2/ZnS Core/Shell Nanocrystals: Cadmium-Free Quantum Dots for In Vivo Imaging, Chem. Mater. 21 (2009) 2422-2429.

[3] E. Luque-Michel, A. Larrea, C. Lahuerta, V. Sebastian, E. Imbuluzqueta, M. Arruebo, M.J. Blanco-Prieto, J. Santamaria, A simple approach to obtain hybrid Au-loaded polymeric nanoparticles with a tunable metal load, Nanoscale (2016).
[4] B. Lasa-Saracibar, M. Guada, V. Sebastian, M.J. Blanco-Prieto, In Vitro Intestinal Co-Culture Cell Model to Evaluate Intestinal Absorption of Edelfosine Lipid Nanoparticles, Curr. Top. Med. Chem. 14 (2014) 1124-1132.
[5] I. Urries, C. Munoz, L. Gomez, C. Marquina, V. Sebastian, M. Arruebo, J. Santamaria, Magneto-plasmonic nanoparticles as theranostic platforms for magnetic resonance imaging, drug delivery and NIR hyperthermia applications, Nanoscale 6 (2014) 9230-9240.
[6] J.R. Cole, N.A. Mirin, M.W. Knight, G.P. Goodrich, N.J. Halas, Photothermal Efficiencies of Nanoshells and Nanorods for Clinical Therapeutic Applications, J. Phys. Chem. C 113 (2009) 12090-12094.
[7] I. Gur, N.A. Fromer, M.L. Geier, A.P. Alivisatos, Air-stable all-inorganic nanocrystal solar cells processed from solution, Science 310 (2005) 462-465.
[8] S.K. Lee, X.Y. Liu, V.S. Cabeza, K.F. Jensen, Synthesis, assembly and reaction of a nanocatalyst in microfluidic systems: a general platform, Lab Chip 12 (2012) 4080-4084.
[9] L. Gomez, V. Sebastian, M. Arruebo, J. Santamaria, S.B. Cronin, Plasmon-enhanced photocatalytic water purification, Phys. Chem. Chem. Phys. 16 (2014) 15111-15116.
[10] A.A. Mikhailovsky, A.V. Malko, J.A. Hollingsworth, M.G. Bawendi, V.I. Klimov, Multiparticle interactions and stimulated emission in chemically synthesized quantum dots, Appl. Phys. Lett. 80 (2002) 2380-2382.
[11] J. Baek, P.M. Allen, M.G. Bawendi, K.F. Jensen, Investigation of Indium Phosphide Nanocrystal Synthesis Using a High-Temperature and High-Pressure Continuous Flow Microreactor, Angew. Chem. Int. Edit. 50 (2011) 627-630.
[12] V. Sebastian, M. Arruebo, J. Santamaria, Reaction Engineering Strategies for the Production of Inorganic Nanomaterials, Small 10 (2014) 835-853.
[13] G.D. Niu, A. Ruditskiy, M. Vara, Y.N. Xia, Toward continuous and scalable production of colloidal nanocrystals by switching from batch to droplet reactors, Chem. Soc. Rev. 44 (2015) 5806-5820.
[14] J.R. Canselier, H. Delmas, A.M. Wilhelm, B. Abismail, Ultrasound emulsification - An overview, J. Disper. Sci. Technol. 23 (2002) 333-349.
[15] I.O.d. Solorzano, L. Uson, A. Larrea, M. Miana, V. Sebastian, M. Arruebo, Continuous synthesis of drug-loaded nanoparticles using microchannel emulsification and numerical modeling: effect of passive mixing, Int. J. Nanomedicine 11 (2016) 3397-3416.
[16] G.T. Vladisavljevic, I. Kobayashi, M. Nakajima, Production of uniform droplets using membrane, microchannel and microfluidic emulsification devices, Microfluid Nanofluid 13 (2012) 151-178.
[17] L. Gomez, V. Sebastian, S. Irusta, A. Ibarra, M. Arruebo, J. Santamaria, Scaled-up production of plasmonic nanoparticles using microfluidics: from metal precursors to functionalized and sterilized nanoparticles, Lab Chip 14 (2014) 325-332.
[18] S. Marre, K.F. Jensen, Synthesis of micro and nanostructures in microfluidic systems, Chem. Soc. Rev. 39 (2010) 1183-1202.
[19] S. Sugiura, M. Nakajima, M. Seki, Effect of channel structure on microchannel emulsification, Langmuir 18 (2002) 5708-5712.

[20] A.A. Maan, K. Schroen, R. Boom, Spontaneous droplet formation techniques for monodisperse emulsions preparation - Perspectives for food applications, J. Food Eng. 107 (2011) 334-346.
[21] S. Santra, P. Zhang, K.M. Wang, R. Tapec, W.H. Tan, Conjugation of biomolecules with luminophore-doped silica nanoparticles for photostable biomarkers, Anal. Chem. 73 (2001) 4988-4993.
[22] S. Freitas, G. Hielscher, H.P. Merkle, B. Gander, Continuous contact- and contamination-free ultrasonic emulsification - a useful tool for pharmaceutical development and production, Ultrason. Sonochem. 13 (2006) 76-85.
[23] E. Phillips, O. Penate-Medina, P.B. Zanzonico, R.D. Carvajal, P. Mohan, Y.P. Ye, J. Humm, M. Gonen, H. Kalaigian, H. Schoder, H.W. Strauss, S.M. Larson, U. Wiesner, M.S. Bradbury, Clinical translation of an ultrasmall inorganic optical-PET imaging nanoparticle probe, Sci. Transl. Med. 6 (2014).
[24] S. Santra, H. Yang, D. Dutta, J.T. Stanley, P.H. Holloway, W.H. Tan, B.M. Moudgil, R.A. Mericle, TAT conjugated, FITC doped silica nanoparticles for bioimaging applications, Chem. Commun. (2004) 2810-2811.
[25] W. Arap, R. Pasqualini, M. Montalti, L. Petrizza, L. Prodi, E. Rampazzo, N. Zaccheroni, S. Marchio, Luminescent Silica Nanoparticles for Cancer Diagnosis, Curr. Med. Chem. 20 (2013) 2195-2211.
[26] A. Burns, H. Ow, U. Wiesner, Fluorescent core-shell silica nanoparticles: towards "Lab on a Particle" architectures for nanobiotechnology, Chem. Soc. Rev. 35 (2006) 1028-1042.
[27] P. Sharma, S. Brown, G. Walter, S. Santra, B. Moudgil, Nanoparticles for bioimaging, Adv Colloid Interfac. 123 (2006) 471-485.
[28] P. Tanury, A. Malhotra, L.M. Byrne, S. Santra, Nanobioimaging and sensing of infectious diseases, Adv. Drug Deliver Rev. 62 (2010) 424-437.
[29] C.L. Chang, H.S. Fogler, Controlled formation of silica particles from tetraethyl orthosilicate in nonionic water-in-oil microemulsions, Langmuir 13 (1997) 3295-3307.
[30] J.Z. Wang, A. Sugawara-Narutaki, M. Fukao, T. Yokoi, A. Shimojima, T. Okubo, Two-Phase Synthesis of Monodisperse Silica Nanospheres with Amines or Ammonia Catalyst and Their Controlled Self-Assembly, Acs Appl. Mater. Inter. 3 (2011) 1538-1544.
[31] S.A. Khan, A. Gunther, M.A. Schmidt, K.F. Jensen, Microfluidic synthesis of colloidal silica, Langmuir 20 (2004) 8604-8611.
[32] L. Gutierrez, L. Gomez, S. Irusta, M. Arruebo, J. Santamaria, Comparative study of the synthesis of silica nanoparticles in micromixer-microreactor and batch reactor systems, Chem. Eng. J. 171 (2011) 674-683.
[33] S. Desgouilles, C. Vauthier, D. Bazile, J. Vacus, J.L. Grossiord, M. Veillard, P. Couvreur, The design of nanoparticles obtained by solvent evaporation: A comprehensive study, Langmuir 19 (2003) 9504-9510.
[34] L. Espanol, A. Larrea, V. Andreu, G. Mendoza, M. Arruebo, V. Sebastian, M.S. Aurora-Prado, E.R.M. Kedor-Hackmann, M.I.R.M. Santoro, J. Santamaria, Dual encapsulation of hydrophobic and hydrophilic drugs in PLGA nanoparticles by a single-step method: drug delivery and cytotoxicity assays, Rsc Adv. 6 (2016) 111060-111069.
[35] X.R. Song, Y. Zhao, S.X. Hou, F.Y. Xu, R. Zhao, J.Y. He, Z. Cai, Y.B. Li, Q.H. Chen, Dual agents loaded PLGA nanoparticles: Systematic study of particle size and drug entrapment efficiency, Eur J. Pharm. Biopharm. 69 (2008) 445-453.

SYNOPSIS